THE JOURNAL OF BIOLOGICAL CHEMISTRY VOL. 282, NO. 47, pp. 34204–34212, November 23, 2007

Probing the Role of PrP Repeats in Conformational Conversion and Amyloid Assembly of Chimeric Yeast Prions*[S]

Received for publication, June 15, 2007, and in revised form, September 11, 2007 Published, JBC Papers in Press, September 24, 2007, DOI 10.1074/jbc.M704952200

Jijun Dong[‡§], Jesse D. Bloom[¶1], Vladimir Goncharov[‡2], Madhuri Chattopadhyay[‖], Glenn L. Millhauser[‖], David G. Lynn[§], Thomas Scheibel[**], and Susan Lindquist[‡3]

*From the [‡]Whitehead Institute for Biomedical Research, Cambridge, Massachusetts 02142, the [§]Department of Chemistry and Biology, Emory University, Atlanta, Georgia 30322, the [¶]Department of Molecular Genetics and Cell Biology, Howard Hughes Medical Institute, University of Chicago, Chicago, Illinois 60637, the [‖]Department of Chemistry and Biochemistry, University of California, Santa Cruz, California 95064, and the **Institut für Organische Chemie und Biochemie, Technische Universität München, D-85747 Garching, Germany*

Oligopeptide repeats appear in many proteins that undergo conformational conversions to form amyloid, including the mammalian prion protein PrP and the yeast prion protein Sup35. Whereas the repeats in PrP have been studied more exhaustively, interpretation of these studies is confounded by the fact that many details of the PrP prion conformational conversion are not well understood. On the other hand, there is now a relatively good understanding of the factors that guide the conformational conversion of the Sup35 prion protein. To provide a general model for studying the role of oligopeptide repeats in prion conformational conversion and amyloid formation, we have substituted various numbers of the PrP octarepeats for the endogenous Sup35 repeats. The resulting chimeric proteins can adopt the [*PSI*$^+$] prion state in yeast, and the stability of the prion state depends on the number of repeats. *In vitro*, these chimeric proteins form amyloid fibers, with more repeats leading to shorter lag phases and faster assembly rates. Both pH and the presence of metal ions modulate assembly kinetics of the chimeric proteins, and the extent of modulation is highly sensitive to the number of PrP repeats. This work offers new insight into the properties of the PrP octarepeats in amyloid assembly and prion formation. It also reveals new features of the yeast prion protein, and provides a level of control over yeast prion assembly that will be useful for future structural studies and for creating amyloid-based biomaterials.

Prions were originally recognized as the causative agent of several mammalian neurodegenerative disorders, including scrapie in sheep, bovine spongiform encephalopathy (mad cow disease) in cattle, and Creutzfeldt-Jakob disease (CJD) in humans (1). According to the prion hypothesis, these maladies are due to a conformational conversion of the normal cellular prion protein (PrP^C)[4] into an abnormal pathological isoform (PrP^{Sc}), a portion of which becomes highly resistant to proteinase-K digestion. Once prion formation is initiated (*i.e.* spontaneous conversion of cellular PrP^C to PrP^{Sc} to generate infectivity), the PrP^{Sc} conformers can self-replicate by templating the conformational conversion of other PrP^C molecules (1). Several prion-like proteins identified in yeast can also perpetuate their conformational states through a protein-based templating mechanism. Instead of causing fatal diseases, however, the yeast prions are sometimes beneficial, and can act as protein-only elements of inheritance (2). For instance, the yeast prion phenotype [*PSI*$^+$] is the result of the self-replicating conformational conversion of the protein Sup35, a translation termination factor. In its prion conformation, Sup35 is sequestered from its normal function, resulting in increased read-through of nonsense codons. This read-through can ultimately confer a wide spectrum of heritable new phenotypes (3–5). *In vitro* the Sup35 prions can form amyloid fibers in a template-based reaction that is thought to parallel *in vivo* prion conformational conversion and is reminiscent of the fiber formation of a wide range of amyloidogenic proteins (2).

The mammalian PrP and yeast Sup35 share several similar structural characteristics, including a well-folded C-terminal core and a natively unfolded N terminus. The N termini of both proteins contain oligopeptide repeats that influence their conformational conversion to the prion state (6–10). The N terminus of wild-type human PrP^C contains four perfect copies of a highly conserved octarepeat sequence (11), PHGGGWGQ, and one imperfect copy, PQGGGTWGQ. Expansion of the octarepeat region, ranging from one to nine extra copies, has been found in several types of familial CJD and is associated with an earlier onset of pathology (12, 13). When transgenic mice that express repeat-free PrP are infected by scrapie extracts or by

* This work was supported in part by a Howard Hughes Medical Institute undergraduate research fellowship (to J. D. B.), National Institutes of Health Grant GM065790 (to G. M. and M. C.), National Institutes of Health Grant GM25874 (to S. L., J. D., and V. G.), the DuPont-MIT alliance, and DOE Grant ER15377 (to J. D. and D. G. L.). The costs of publication of this article were defrayed in part by the payment of page charges. This article must therefore be hereby marked "*advertisement*" in accordance with 18 U.S.C. Section 1734 solely to indicate this fact.

[S] The on-line version of this article (available at http://www.jbc.org) contains supplemental Figs. S1–S5.

[1] Present address: Division of Chemistry and Chemical Engineering, California Institute of Technology, Pasadena, CA.

[2] Present address: Francis Bitter Magnet Laboratory/MIT, Cambridge, MA.

[3] An investigator of the Howard Hughes Medical Institute. To whom correspondence should be addressed: Whitehead Institute for Biomedical Research, Cambridge, MA 02142-1479. Tel.: 617-258-5184; Fax: 617-258-7226; E-mail: lindquist_admin@wi.mit.edu.

[4] The abbreviations used are: PrP^C, cellular prion protein; PrP^{Sc}, pathological isoform of cellular prion protein; EPR, electron paramagnetic resonance; YPD, yeast peptone dextrose medium; AFM, atomic force microscopy; ThT, Thioflavin T; GST, glutathione *S*-transferase; MOPS, 4-morpholinepropanesulfonic acid; AFM, atomic force microscopy; ThT, thioflavin-T; SOD, superoxide dismutase.

PrP aggregates, they show a slower progression of disease (9, 14) and exhibit different histopathological characteristics than mice with the wild-type protein (15). *In vitro*, expansion of the octarepeat region increases the spontaneous conversion rate of PrP^{C} to a protease-resistant conformation (16). Likewise, when the octarepeat region is fused to a GST (glutathione *S*-transferase) protein, it accelerates protein self-association and allows selective binding of PrP^{Sc} from brain extracts (17). Sup35 has five imperfect copies of PQGGYQQYN. Reducing the number of repeats lowers the frequency of spontaneous prion induction (7, 18). Furthermore, the prion state associated with this variant is unstable and frequently spontaneously converts back to the non-prion state, [psi^{-}] (7). Sup35 with an expanded number of repeats, however, induces a new and stable prion state much more frequently than wild-type Sup35 (7).

Oligopeptide repeats of various lengths and compositions appear in several other amyloid-forming proteins in addition to prion proteins. The huntingtin protein associated with Huntington's disease contains a perfect polyglutamine repeat, and expansion of this repeat region results in early onset of the disease and an increase in the rate of *in vitro* amyloid formation (19, 20). α-Synuclein, a protein that plays a role in Parkinson disease and assembles into amyloid fibers *in vitro*, contains seven copies of a less defined repeat, *X*KTKEGV*XXXX* (21). The major and minor components of the *Escherichia coli* curli protein each consist of five 16–18 mer repeats, which are required for the formation of curli amyloid fibers and are involved in cell aggregation, biofilm formation, and surface adhesion (22, 23). Although oligopeptide repeats are clearly a crucial feature of these amyloid-forming proteins, the exact structural and functional role of these repeats remains unclear.

Compared with these other oligopeptide repeats, the biophysical properties of the PrP octarepeats are well characterized. The octarepeat of PrP can selectively bind Cu(II) ions (24), and the histidine residues in the octarepeats act as the primary anchor point for Cu(II) binding (24). Structurally, Cu(II) binding can induce a conformational conversion of PrP^{C} into protease-resistant species (10), and the efficiency of this conversion depends on the number of octarepeats (17). Cu(II) ions combined with nicotinamide adenine dinucleotide phosphate (NADPH) can even induce spontaneous conformational change and aggregation of HuPrP-(23–98), a variant that only contains the octarepeat region of human PrP (25). Functionally, Cu(II) binding to the octarepeats induces PrP^{C} endocytosis in neuronal cells, indicating a role for PrP^{C} in Cu(II) sensing, uptake and/or transport (26). Superoxide dismutase (SOD)-like activities have also been reported for the Cu(II)-bound PrP^{C}, suggesting a neuronal function of PrP^{C} as an anti-oxidant (27–29), although that is still a subject of debate (30). Treatment of scrapie-infected mice with Cu(II) chelator D-(−)-penicillamine (D-PEN) delays the onset of prion disease in mice (31).

While the biophysical properties of the PrP repeats have been studied extensively, the role of the repeats in prion conformational conversion is not well understood, particularly because of the lack of knowledge on many details of PrP prion formation. One the other hand, the factors that guide prion conformational conversion have been best defined for Sup35. These factors include molecular chaperones that influence conformational conversion (32–35), as well as specific sequence elements that control the maintenance and nucleation of the prion conformation and govern the formation of distinct prions strains and the existence of prion species barriers (36–40). To provide a new model for studying prion conformational conversion and to better understand the role of the oligopeptide repeats in amyloid formation, we explored the role of the PrP octarepeats in the context of the yeast prion protein Sup35. We created chimeric proteins in which different numbers of hamster PrP repeats were substituted for the endogenous Sup35 repeats. Facilitated by the powerful genetic and biophysical techniques developed for yeast prions, we were able to characterize how the PrP octarepeats influence the conformational conversion and amyloid formation of these chimeric prion proteins both *in vivo* and *in vitro*.

We find that increasing the number of PrP repeats in the chimeric proteins increases the spontaneous appearance of the [PSI^{+}] phenotype *in vivo* and accelerates amyloid formation *in vitro*. Conformational conversion and amyloid formation by the chimeras are modulated by both pH and the presence of metal ions. Further, the manner in which these factors modulate conversion is highly sensitive to the number of PrP repeats. Our work offers new insight into the role of the PrP octarepeats in amyloid formation and prion formation, with implications for prion structure. It also allows us to control protein assembly by simply altering environmental conditions. This control will be useful for further functional and structural work and could provide a practical means of controlling assembly for biomaterial and biotechnology applications.

EXPERIMENTAL PROCEDURES

Plasmid Construction and Gene Integration—A Sup35 integrative vector was constructed using pRS306 (41). A fragment spanning from 1360 nucleotides upstream of Sup35 through a 5′-region of Sup35 with a BspE1 site after the first Sup35 repeat was amplified (PCR primers 5′-CGACGGTATCGATAAGCTTG-3′ and 5′-GATAGCCTCTAGATTGGTATCCGGAATAACCTTG-3′) and ligated into pRS306 between ClaI and XbaI sites. A second fragment spanning from Sup35 downstream from the repeats with an EagI site just after the repeats to 800 nucleotides downstream from Sup35 was amplified (PCR primers 5′-CAGCAATCTAGACCACAAGGCGGCCGTGGAAATTAC-3′ and 5′-CGAATTGGAGCTCTTACTCG-3′) and ligated into the plasmid between XbaI and SacI sites. This plasmid was sequenced through the entire Sup35 region, and was named pRS306Sup35R1.

The first two PrP repeats were added to pRS306Sup35R1 by annealing two complementary oligonucleotides and inserting them between the BspE1 and EagI sites. To ensure high purity of these lengthy oligos, they were ordered PAGE-purified and phosphorylated from Research Genetics (oligo sequences 5′-CCGGATATCCACAAGGTGGAGGTACTTGGGGTCAACCCCATGGAGGTGGTTGGGGTCAACCACAAGGC-3′ and 5′-GGCCGCCTTGTGGTTGACCCCAACCACCTCCGGGTTGACCCCAAGTACCTCCACCTTGTGGATAT-3′), and contained a BstXI site. The resulting plasmid was named pRS306Sup35R1+2. Subsequent repeats were added by inserting annealed oligos encoding three PrP

repeats in the BstXI site (oligo sequences 5′-GAGGTTGGGGTCAACCCCATGGAGGAGGTTGGGGTCAACCCCATGGAGGTGGTTGGGGTCAACCCCATGGAG-3′ and 5′-ATGGGGTTGACCCCAACCACCTCCATGGGGTTGACCCCAACCTCCTCCATGGGGTTGACCCCAACCTCCTCC-3′). The addition of one copy of these annealed oligos created pRS306Sup35R1+5. The oligos contained two BstXI sites, so digestion with BstXI and self-ligation created pRS306Sup35R1+4, while digestion with BstXI and insertion of another copy of the annealed oligos created pRS306Sup35R1+7. In a similar manner, pRS306Sup35R1+6 and pRS306Sup35R1+8 were created. All of these plasmids were sequenced through the repeat region to confirm accuracy.

The plasmids for the R1+8H1Q chimera were created by the same method, inserting oligos encoding PrP repeats in which the histidines were changed to glutamines into pRS306Sup35R1+2 (oligo sequences 5′-GAGGTTGGGGTCAACCC CAAGGAGGAGGTTGGGGTCAACCCCAAGGAGGTGGTTGGGGTCAACCCCAAGGAG-3′ and 5′-TTGGGGTTGACCCCAACCACCTCCTT GGGGTTGACCCCAACCTCCTCCTTGGGGTTGACCCCAACCTCCTCC-3′). The plasmids pRS306Sup35R1+8H1Q was created in this manner and sequenced through the repeat region. Note that these plasmids still contained the one histidine that was present in the repeats in pRS306Sup35R1+2.

Bacterial expression constructs for R1+4, R1+8, and R1+8H1Q were created by excising the repeat region from the corresponding integration constructs with BstEII and MscI and ligating it into these sites in the expression construct pJC25NMstop (42). These constructs were named pJC25R1+4stop, pJC25R1+8stop and pJC25R1+8H1Q. These plasmids were sequenced through the repeat region to confirm accuracy.

Gene Integration and Replacement—The integration constructs were linearized with MluI and transformed into a [*psi*$^-$] 74-D694 (genotype: ade1–14(UGA), trp1–289(UAG), his3Δ-200, ura3-52, leu2-3,112) strain. Transformants were selected on uracil-deficient medium (S.D.-Ura), and recombinant excision events were selected on medium containing 5-fluoroorotic acid. Strains in which the wild-type Sup35 gene had been replaced by the mutant copy were identified by PCR of a portion of the genomic Sup35 gene. The repeat region of the Sup35 gene was sequenced to confirm accuracy.

Spontaneous Appearance of [PSI$^+$] in R1+X Yeast Strains—All R1+X strains were grown on YPD plates, and then inoculated in liquid YPD. After overnight growth, the cells were plated on ADE− at 0.7×10^6, 1.4×10^6, and 6×10^6 cells/plate. After 7 days of incubation, colonies were counted.

Protein Purification—Crude preparations of proteins were purified as previously described (43). Mass spectrometry analysis yielded the following masses: R1+4 was 27171.1 Da (calculated value is 27170.1 Da), R1+8 was 30277.6 Da (calculated value is 30277.3Da), and R1+8H1Q was 30222.9 Da (calculated value is 30223.3 Da). Protein concentrations were determined using the absorbance at 280 nm with molar extinction coefficients calculated as 25,600 (NM), 39400 (R1+4), 62160 (R1+8), and 62160 (R1+8H1Q).

Fiber Formation—Proteins were dissolved in 6 M guanidine hydrochloride as a stock solution, and the concentration was determined by the absorbance at 280 nm. Solutions for unseeded polymerization reactions were prepared by dilution of the stock solution into aqueous buffers and allowed to assemble at room temperature either with our without agitation. Seeds for seeded reactions were prepared by sonicating preformed fibers in a VWR Aquasonic 50T water bath sonicator, and all seeded reactions contained 2% (w/w) of the seeds.

The buffers for the tests at different pH values are: pH 7.2, 20 mM MOPS with 100 mM sodium chloride; pH 6.2, 5 mM potassium phosphate with 50 mM sodium sulfate; pH 4.9, 3.9, and 2.9, 5 mM potassium acetate with 50 mM sodium sulfate.

Cu(II) Binding Reactions—Lyophilized protein was first dissolved in acidified 25 mM NEM, 300 mM NaCl and spin filtered through a 300 kDa cutoff membrane. An appropriate volume of 100 mM $CuCl_2$ in deionized water was added and samples were mixed. Then samples were diluted to 5–20 μM final protein concentration using 30 mM NEM pH 8.1. All EPR samples contained 20% (v/v) glycerol as a cryoprotectant.

Electron Spin Resonance Spectroscopy—X-band spectra (9.43 GHz) were acquired using a Bruker ELEXSYS E500 spectrometer and a TE_{102} cavity. Measurements were performed at ~115–125K in a nitrogen vapor using cavity equipped with variable temperature control. The total bound Cu(II) was quantified by spin integration and comparison to accurate standard solutions containing Cu(II) in 10 mM imidazole at pH 7.4.

Thioflavin-T Binding—Fiber formation was monitored by Thioflavin-T (44) in both seeded and unseeded reactions (45). Attenuated Thioflavin T (ThT) intensity was observed at acidic pHs and in the presence of Cu(II), when SDS assay showed the same amount of free monomers left after polymerization reactions. ThT fluorescence intensity was baseline subtracted and then normalized to the maximum intensity when the polymerization reaction reached equilibrium.

Monitoring Fiber Formation by SDS Solubility—At the indicated time points, 20 μl of the assembly mix was withdrawn and added to SDS-PAGE sample buffer. Samples were run on 12.5% SDS-PAGE gels and stained with Coomassie Blue G-250. The percentage of soluble protein was calculated by (gel band intensity at indicated time point) divided by (gel band intensity of zero hour sample after boiling).

RESULTS

Chimeric Sup35 Proteins with PrP Repeats Can Support Both the Prion and Non-prion States—We first constructed chimeric proteins consisting of Sup35 with different numbers of PrP repeats substituted for the repeats of Sup35. Because the first repeats of Sup35 and PrP are the least similar to each other in sequence, and since the first Sup35 repeat is spatially separated from the others, we kept it intact. The last four full Sup35 repeats were replaced with the repeats from hamster PrP: one copy of the first hamster PrP imperfect repeat (PQGGGTWGQ) followed by varying numbers of the perfect hamster PrP repeats (PHGGGWGQ), as shown in Fig. 1*A*. Because our chimeras contained the first repeat (R1) of Sup35 plus two, four, five, six, seven, and eight repeats, they were named R1+2, R1+4, R1+5, R1+6, R1+7, and R1+8.

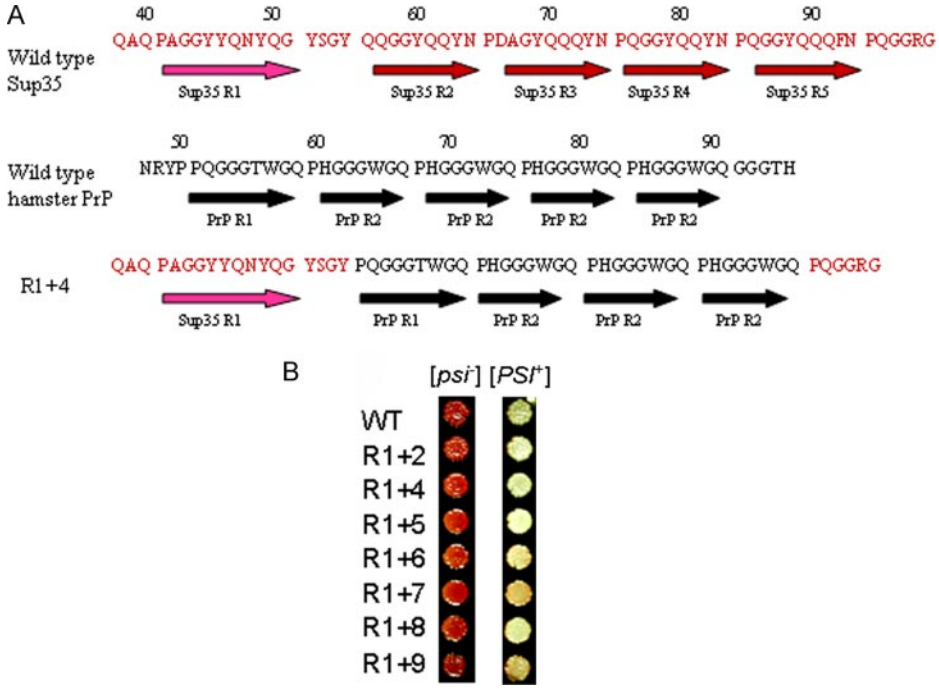

FIGURE 1. *A*, replacement of the Sup35 repeats with repeats from PrP. The last four repeats of wild-type Sup35, spanning residues 56–93, were replaced by the first repeat from hamster PrP and then various numbers of copies of the second repeat from hamster PrP. Chimeric proteins therefore contained the first Sup35 repeat plus 2, 4, 5, 6, 7, and 8 PrP repeats, and so were named R1+2, R1+4, R1+5, R1+6, R1+7, and R1+8. The amino acids from the Sup35 sequence are in *red*, and those from PrP are in *black*. *B*, all of the R1+X chimeras supported both [*PSI*$^+$] and [*psi*$^-$] states. The strains were spotted on YPD.

We first asked how these chimeric proteins affected yeast prion biology *in vivo*. Starting with [*psi*$^-$] cells, the wild-type *SUP35* gene was replaced with a gene encoding R1+2, R1+4, R1+5, R1+6, R1+7, or R1+8 by homologous recombination. The strain we employed contains a nonsense codon in the *ADE1* gene. In [*PSI*$^+$] cells, wherein most of the Sup35 translation termination factor is sequestered in prion aggregates, ribosomes sometimes read through the stop codon. This allows the cells to grow on adenine deficient media (S.D.-Ade) and causes them to form white colonies when grown on rich media (YPD) (46, 47). The [*psi*$^-$] cells do not grow on S.D.-Ade, and produce red colonies on YPD because of the accumulation of a metabolic by-product of adenine biosynthesis (46). Strains in which wild-type Sup35 was replaced with R1+2 through R1+8 substitutions remained [*psi*$^-$].

Increasing the Number of PrP Repeats Destabilizes Both the [psi$^-$*] and [PSI*$^+$*] States*—When wild-type cells are grown in YPD, they are stable in both the [*PSI*$^+$] and the [*psi*$^-$] states, and the rate of spontaneous conversion between these states is very low (7). To determine the stability of the [*psi*$^-$] state in our mutant strains, we observed the spontaneous appearance of [*PSI*$^+$] by streaking [*psi*$^-$] cells on YPD followed by an S.D.-Ade plate. Wild-type Sup35 [*psi*$^-$] strains produced colonies on S.D.-Ade medium rarely, approximately one per 10^6 cells/plate. R1+2, R1+4, R1+5, also rarely produced colonies. In contrast, colonies appeared ~10-fold more frequently on S.D.-Ade medium with R1+6 and ~100-fold more frequently with R1+7 and R1+8 strains. The colonies were confirmed as being true [*PSI*$^+$] colonies by taking advantage of the fact that cells can be cured of the prion state by growing them on media containing guanidine hydrochloride. This produced red colonies that could not grow on S.D.-Ade medium. Thus, repeat expansion increased rate of spontaneous conversion from the [*psi*$^-$] to the [*PSI*$^+$] state.

Next we examined the spontaneous conversion of R1+X [*PSI*$^+$] strains to [*psi*$^-$]. To create [*PSI*$^+$] strains of R1+2, R1+4, R1+5, and R1+6, large numbers of the [*psi*$^-$] strains were plated on S.D.-Ade and colonies that grew were selected. All of the [*PSI*$^+$] strains were confirmed by growth and curing in the presence of 5 mM Gdn·HCl. Fig. 1*B* shows the growth of R1+X strains in both [*psi*$^-$] and [*PSI*$^+$] states on YPD. When R1+2, R1+4, R1+5, and R1+6 [*PSI*$^+$] strains were grown on YPD-rich medium, the colonies appeared white, and red colonies were rarely observed, similar to wild-type Sup35 [*PSI*$^+$] strains. Thus, the [*PSI*$^+$] states of R1+2, R1+4, R1+5, and R1+6 were maintained stably. However, R1+7 and R1+8 strains frequently converted to [*psi*$^-$] on YPD plates, with the colonies sectoring to red around the perimeter. Thus, extra copies of the PrP octarepeats destabilize both the prion and non-prion states.

Increasing the Number of PrP Repeats Dramatically Accelerates Amyloid Formation in Vitro—Sup35 can be divided into three distinct regions, the N terminus with the oligopeptide repeats (amino acids 1–123), a highly charged middle region, and the C terminus (amino acids 254–685), which functions as a translation termination factor. The N terminus (N) and the middle region (M) of Sup35, often called NM, forms the prion-determining (PrD) domain. *In vitro* assembly of NM amyloid fibers recapitulates the induction and propagation of yeast prions *in vivo* (7, 39, 48, 49), and transformation of NM fibers into [*psi*$^-$] yeast cells (50) induces the formation of yeast prion phenotypes (36, 39, 48). To examine the amyloidogenic properties of the R1+X proteins, we chose to purify the NM domains of wild-type Sup35, R1+4, and R1+8. Amyloid fibers formed by the R1+4 and R1+8 chimeras were examined by atomic force microscopy (AFM). They were morphologically indistinguishable from those formed by wild-type NM (supplemental Fig. S1).

The kinetics of amyloid formation were monitored both by a Thioflavin-T (ThT) binding assay and by an assay for resistance to solubilization by SDS (46). Wild-type NM or chimeric NMs were diluted from a 6 M Gdn·HCl stock solution into aqueous buffer and incubated at room temperature with agitation, a standard condition that accelerates assembly. Under these conditions, all of the proteins exhibited behavior typical of spontaneous, nucleated amyloid formation, with an initial lag phase followed by an assembly phase (Fig. 2*A*). However, wild-type

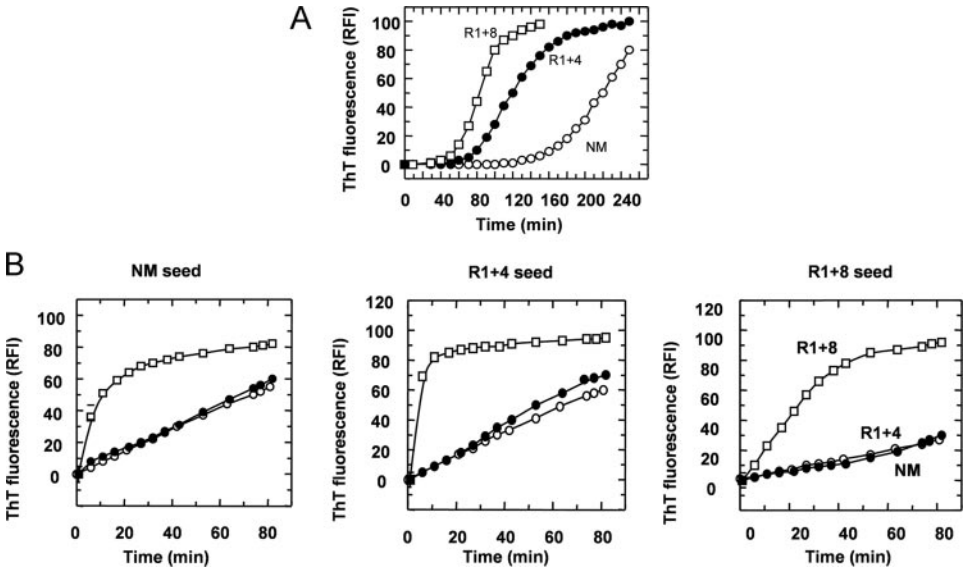

FIGURE 2. **Proteins form amyloid fibers with a lag phase that is eliminated by the addition of pre-formed fiber seeds, as monitored by ThT binding.** *A*, in unseeded reactions, proteins with more repeats form amyloid fibers with a shorter lag phase. *B*, lag phase for fiber formation is eliminated for all proteins by the addition of 2% (w/w) pre-formed fibers from any of the other proteins. All reactions use 5 μM solutions of soluble proteins of the NM domains of wild-type Sup35 (*open circles*), R1+4 (*filled circles*), and R1+8 (*open squares*). Polymerization reactions were performed at room temperature under gentle rotation conditions. ThT fluorescence intensity was normalized to the maximum intensity when the polymerization reaction reached an equilibrium determined by both the ThT and SDS-PAGE assays.

NM and the chimeras exhibited very different lag times. Both chimeras with PrP repeats showed a shorter lag phase than wild-type NM. Moreover, R1+8 exhibited a shorter lag phase than R1+4. These experiments were performed many times with independent protein preparations. Although the absolute lag times varied somewhat from experiment to experiment, the differences between the behavior of three proteins were extremely consistent. This result indicates that the PrP octarepeat is more amyloidogenic than the Sup35 repeat, and that the number of PrP octarepeats can greatly alter the intrinsic capacity of the proteins to form amyloid.

To test the effects of the PrP repeats on the assembly phase of amyloid formation, seeded polymerization reactions were monitored. Pre-formed NM fibers seeded fiber formation of wild-type NM with elimination of the lag phase (46) (Fig. 2*B*). Wild-type NM fibers also effectively seeded fiber formation of R1+4 and R1+8 (2% w/w seed, Fig. 2*B*). Moreover, all three proteins were able to effectively cross seed each other (Fig. 2*B*). In all seeded reactions and regardless of the nature of the seeds R1+8 assembled much faster than R1+4 and wild-type NM. These findings were confirmed by SDS resistance assay (data not shown). Thus, the number of the PrP repeats influences both the spontaneous nucleation rate and the inherent assembly rate of amyloid formation. But strikingly, the repeats have little effect on seeding or cross-seeding capacity.

Histidine Residues in the PrP Repeats Confer pH Sensitivity on Amyloid Formation—We then explored the factors that may affect the conformation of the repeat region and thereby the process of amyloid formation. Previous studies showed that conformational conversion of truncated PrPs free of the repeat region was sensitive to pH (51–53) and the remaining histidine residues in the truncated PrP were suggested to be crucial for this pH sensitivity (54). To our knowledge, the role of histidines in the octapepetide repeats has not been well tested. To examine the effect of pH on the spontaneous assembly of the chimeras, we used quiescent reaction conditions, which extend the lag phase. Amyloid formation by wild-type NM, R1+4 and R1+8 in buffers with different pH values was monitored by both ThT (Fig. 3*A*) and SDS (supplemental Fig. S2) assays. The lag phase of wild-type NM was insensitive to pH, with similar amyloid formation time courses at pH 7.2, 6.2, 4.9, 3.9, and 2.9. In contrast, lowering the pH lengthened the lag phase for both R1+4 and R1+8, with the effect especially profound for R1+8. The lag phase for R1+8 was less than 2 h at pH 7.2 and 6.2, but it was more than 10 h at pH 4.9 and more than 30 h at pH 2.9. We also investigated the effects of pH on seeded assembly (Fig. 3*B* and supplemental Fig. S3). The assembly rate of wild-type NM remained almost unchanged. However, the assembly rate of R1+4 and R1+8 decreased at lower pH. Moreover, R1+8 was more sensitive to pH changes than R1+4, particularly at pH 4.5.

To directly test whether the histidine residues are responsible for the pH dependence of assembly, we mutated the histidines in the repeat region of R1+8 to glutamines (changing PHGGGWGQ to PQGGGWGQ). Glutamine was chosen since it is present in the first imperfect repeat (PQGGGTWGQ) in the same location as the histidine in the subsequent PHGGGWGQ repeats (Fig. 1*A*). Because of details of the cloning procedure, the histidine was not removed from the second PrP repeat. Therefore, this new chimera contained only a single PrP repeat with histidine, and was named R1+8H1Q. The histidine replacement had no obvious effect on the function of the protein *in vivo*: R1+8H1Q strains supported both [*PSI*$^+$] and [*psi*$^-$] states, and the purified NM domain of R1+8H1Q formed amyloid fibers *in vitro* (supplemental Fig. S1). However, unlike the R1+4 and R1+8 proteins with histidines in the repeats, both the spontaneous nucleation rate and the assembly rate for amyloid formation by R1+8H1Q was almost unchanged across the entire tested pH range, from pH 7.2 to 2.9 (Fig. 3, *A* and *B*). Thus, the histidine residues are the primary source of the pH sensitivity of amyloid formation by the R1+4 and R1+8 proteins.

Interplay between Cu(II) and PrP Repeats Shows Complex Effects on Amyloid Formation in Vitro—It has been extensively shown that the PrP repeats can selectively bind Cu(II) ions (24, 55–58). Therefore, we explored the effect of Cu(II) on the conformational conversion and amyloid formation of the chimeras. First, we investigated the Cu(II)-binding sites in non-assembled NM and R1+X proteins by Electron Paramagnetic Resonance (EPR). EPR has been previously applied to determine the

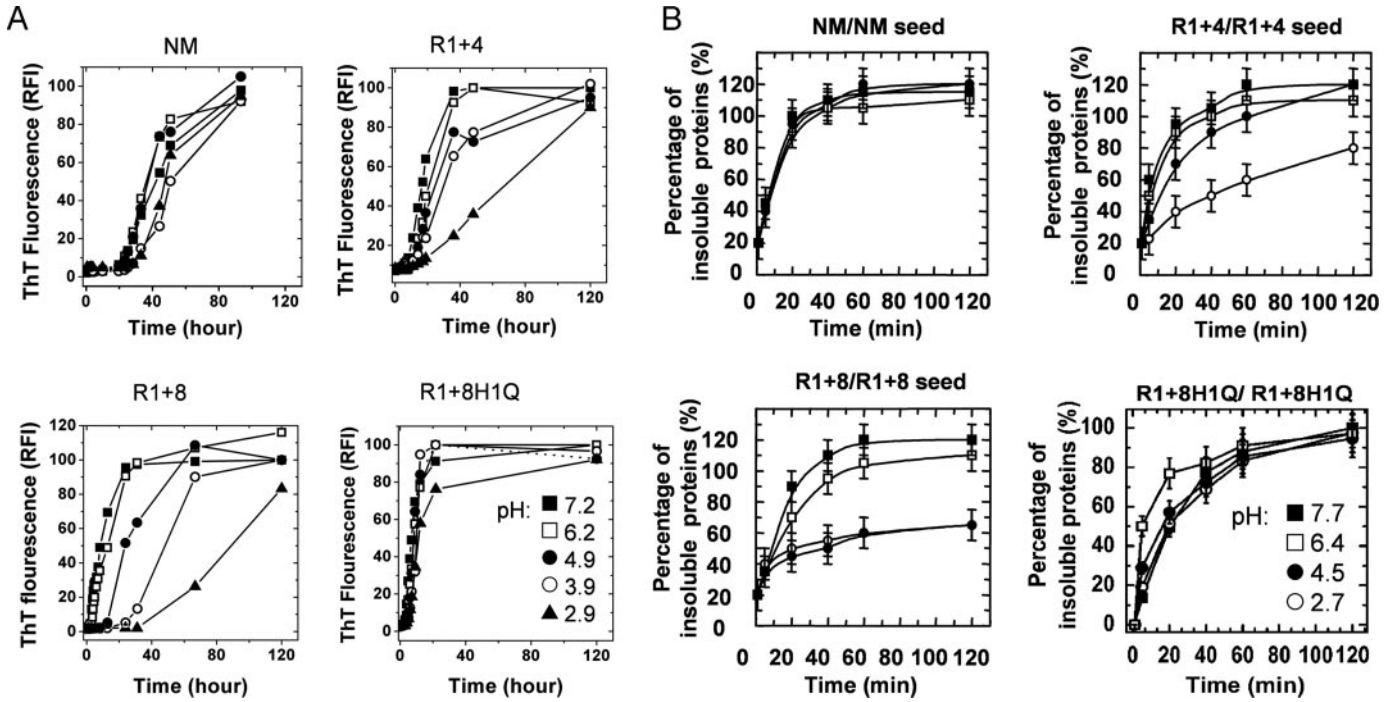

FIGURE 3. *A*, lag times of amyloid formation for the R1+X proteins and wild-type NM showed different sensitivities to pH, as monitored by the ThT binding assay. The graphs show fiber formation in 5 μM solutions of the NM domains of wild-type Sup35, R1+4, R1+8, and R1+8H1Q at room temperature without rotation. The reactions were carried out at pH 2.9 (*filled triangle*), 3.9 (*open circles*), 4.9 (*filled circles*), 6.2 (*open squares*), and 7.2 (*filled squares*). *B*, propagation of amyloid fibers of the R1+X proteins is affected by pH, as monitored by SDS assay. The *graphs* show the assay for fiber formation in 2.5 μM solutions of the NM domains of wild-type Sup35, R1+4, R1+8, and R1+8H1Q with 2% (w/w) of seed from the same protein type. The reactions were carried out at pH 2.7 (*open circles*), 4.5 (*filled circles*), 6.4 (*open squares*), and 7.7 (*closed squares*).

molecular features of the Cu(II)-binding sites in recombinant full-length Syrian hamster PrP^C (59). Those results showed that Cu(II) coordination depends highly on the relative concentration of Cu(II) to PrP^C (60). With excess amount of Cu(II), copper fully occupies individual repeat units, one Cu(II) per repeat unit, coordinating with the His imidazole and two deprotonated glycine amides (59, 61). The EPR spectra of Cu(II)-bound R1+4 and R1+8 are nearly indistinguishable from that of Cu(II)-bound recombinant PrP^C at full occupancy (60), although in R1+8 there may be additional broadening in the parallel region (~2700 G–3100 G; Fig. 4). This broadening is possibly due to Cu(II)-Cu(II) dipolar interactions. On average, R1+4 bound 4–5 equivalents of Cu(II), and R1+8 bound up to 10 equivalents. Wild-type NM and R1+8H1Q bind Cu(II) at ~2 and 4 equivalents, respectively. They might bind Cu(II) via histidine residues outside the octarepeat region, and/or the free amino group at the N terminus. R1+8H1Q retains a single histidine-containing repeat, which is also likely responsible for the additional Cu(II) binding compared with wild-type NM.

We then investigated the effects of Cu(II) on amyloid formation by the R1+X chimeras. 10 equivalents of Cu(II) were added into NM and R1+4 solution, and 20 equivalents were added into R1+8 and R1+8H1Q. As a result, the ratio of [Cu(II)]/[single repeat] is constant, eliminating a variable that influences Cu(II) coordination environment (60). Formation of amyloid fibers of all R1+X proteins and NM in the presence of Cu(II) was confirmed by AFM, morphologically similar to that formed in the absence of Cu(II) (supplemental Fig. S4). By the ThT assay, Cu(II) had no obvious effect on the assembly of wild-type NM, but it did affect the lag phase

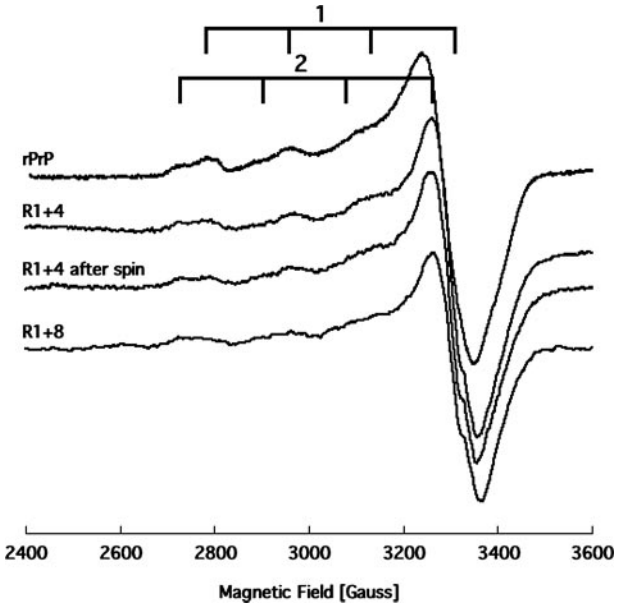

FIGURE 4. **EPR spectra of recombinant PrP^C, R1+4, and R1+8 fully loaded with Cu(II).** R1+4 and R1+8 reveal binding components 1 and 2 (parallel hyperfine features labeled) indistinguishable from those observed for recombinant PrP^C. The recorded spectra are from monomeric protein in complex with Cu(II), because centrifugation to remove aggregates (after spin) did not alter the spectral features. Samples were prepared in 27.5 mM NEM, 150 mM NaCl, pH 7.7.

of fiber formation by the chimeric NMs (Fig. 5). For R1+4, the presence of 10 equivalents of Cu(II) slightly accelerated assembly. In contrast, Cu(II) showed an opposite effect on R1+8, reducing assembly by increasing the lag phase by

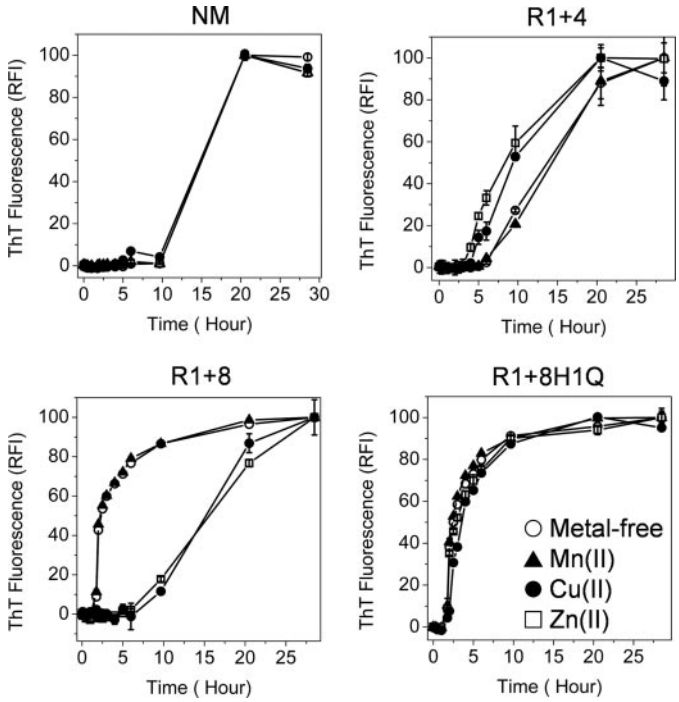

FIGURE 5. **Different divalent metal ions [Cu(II), Zn(II), and Mn(II)] showed different effects on the lag phase of amyloid formation by the wild-type NM, R1+4, R1+8, and R1+8H1Q, as monitored by ThT binding.** Metal ions were added in 10 equivalents for NM and R1+4 and in 20 equivalents for all other proteins. Polymerization reactions were performed at room temperature with a gentle shaking at 600 rpm. Metal ion-free samples (*open circle*), samples containing Cu(II) (*solid circle*), Zn(II) (*open square*), and Mn(II) (*solid triangle*).

about a factor of 2. (This surprising difference in the effects of Cu(II) was confirmed on independent protein preparations by two investigators, V.G. and J.D.) Cu(II) showed no effect on the lag phase of R1+8H1Q fiber formation. Thus, Cu(II) must modulate the lag phase of R1+8 amyloid assembly by interacting with the histidine residues of the PrP repeats. Results obtained with Thioflavin T fluorescence were confirmed by the SDS-resistance assay (supplemental Fig. S5).

Recombinant PrP^C binds to Cu(II), Zn(II), and Ni(II), but has no detectable interaction with other metals, such as Mn(II) (55, 57, 58). To test the specificity of Cu(II) on the R1+X proteins, we examined the effects of Zn(II) and Mn(II) on amyloid formation of R1+4 and R1+8. Both ThT binding (Fig. 5) and SDS assay (supplemental Fig. S5) showed that, as expected from the binding selectivity, Mn(II) did not affect the lag phase of fiber formation for either protein. Zn(II), however, modulated fiber formation of R1+4, R1+8, and R1+8H1Q with the same trend as Cu(II), increasing the lag phase of R1+8 amyloid formation, decreasing the lag phase of fiber formation of R1+4, and having no effect on R1+8H1Q. Thus, the effects of metal ions on the polymerization of the R1+X proteins reflect how the ions rank in their selectivity of binding to recombinant PrP^C (55, 57, 58).

DISCUSSION

To provide a model system for studying oligopeptide repeats in amyloidogenic proteins, we replaced the oligopeptide repeats of Sup35 with the well-characterized octarepeats of PrP. The resulting chimeric proteins allowed us to characterize the properties of the PrP repeats in the context of both yeast prion formation and amyloid assembly. The chimeric proteins are fully capable of supporting the induction and maintenance of the yeast [PSI^+] phenotype. R1+4, the chimera with the same number of repeats as wild-type NM, forms amyloid fibers more rapidly than NM, establishing that the PrP octapeptide repeats are more amyloidogenic than Sup35 repeats. Expanding the number of PrP repeats greatly increases the rate of amyloid assembly *in vitro* and the spontaneous appearance of [PSI^+] *in vivo*. We previously showed that expanding the number of endogenous Sup35 repeats accelerates amyloid formation and increases the spontaneous rate of [PSI^+] appearance (7). Thus, the two types of repeats have a very similar effect on amyloid conformational conversion and on yeast prion biology.

Curiously, expanding the number of repeats destabilized the [PSI^+] and [psi^-] states, increasing switching in both directions. Both results can be explained by our finding that R1+8 is more amyloidogenic than R1+4. In destabilizing the [psi^-] state, it seems most likely that R1+8 simply converts spontaneously into the amyloid prion state, [PSI^+], more frequently than does R1+4. But how might a greater propensity to form an amyloid destabilize the [PSI^+] state? There are at least two likely possibilities based on our current findings. First, R1+8 amyloids may be too stable to be severed by Hsp104 for efficient transmission to daughter cells. A reduced partitioning rate would lead to the loss of [PSI^+] (62). Second, the increased efficiency of amyloid conversion might sequester too much of the Sup35 essential translation-termination activity. This would provide a selective advantage to cells that switch to the [psi^-] state. A third, alternative explanation is that the repeats interact with Hsp104 leading to increased disassembly of the prion (18).

In any case, the strong effects of repeat expansions are intriguing. We previously proposed that [PSI^+] provides a mechanism for cells to switch heritably between distinct phenotypic states (63, 64). It may be that the number of repeats in Sup35, and the degree of their amyloidogenicity, has been subject to evolutionary pressures to optimize switching rates according to the frequency of environmental change.

The model substrates we have created allow multiple methods for interrogating the ways in which repeats can influence amyloid formation. As shown for wild-type NM, a collapsed oligomeric intermediate facilitates the intermolecular contacts required for nucleation (32, 36, 40, 65). In our chimeras, the structures populated by the collapsed intermediate can be modulated by the number of repeats, by pH and by metal ions, and each of these factors dramatically influences the lag time of unseeded polymerization. Thus, these substrates, together with new methods of single molecule fluorescence (66), should provide powerful new tools to study the biophysics of conformational conversion, both in nucleation and polymerization.

Indeed, results from the initial analysis reported here already have interesting implications. First, although wild-type NM and R1+4 have very different spontaneous nucleation rates they have virtually identical seeded polymerization rates. The increased amyloidogenicity of R1+4 compared with NM, then, is solely due to a change in spontaneous nucleation. Second,

R1+4 and NM have much slower rates of seeded polymerization than R1+8. Third, and most strikingly, these very different rates of seeded polymerization are independent of the seed. That is, seeds formed by R1+8, by R1+4, or by wild-type NM cross-seed polymerization of all three proteins in the very same way. These results fit well with one structural model for NM fibers, but not another. In the model proposed by Shewmaker *et al.* (67), the residues of the N domain stack upon each other, with the repeat region forming an extensive intermolecular interface. Under this model, it would be hard to understand why replacing 38 amino acids (out of 123) in the N domain with 64 heterologous amino acids from the PrP protein, has virtually no effect on cross seeding activity. In the second model by Krishnan *et al.* (36), the repeat region is largely sequestered from intermolecular contacts. The repeats are envisioned as coiling upon each other during amyloid formation, which would be consistent with facilitated nucleation we observe with expanding the repeats. However, intermolecular contacts are primarily made by flanking regions in this model (36). Efficient cross-seeding between wild-type NM and the two chimeras would therefore be expected, since they contain the same sequences in the flanking regions for inter-molecular contacts (36, 40, 65).

Further study of these chimeric proteins might also help us understand the effects of the PrP repeats, pH and metal ions, on prion initiation by wild-type PrP. Although the repeats are outside the main amyloid core of PrP and lie within it in NM, their collapse into a compact, molten folding intermediate might affect PrP and NM nucleation in a similar way, by freeing flanking regions to make their critical nucleating contacts. Acidic conditions facilitate the conversion of the C-terminal segment of PrP^{C} into aggregation-prone conformations (51–53), while the pH dependence of full-length PrP is not well established. Our chimeric proteins show decreased assembly rates under acidic conditions, and this effect is profound for proteins with repeat expansions. Such pH sensitivities may be of importance in disease since one compartment that might be involved in the conversion of PrP^{C} to PrP^{Sc} is the acidic endosome (68, 69). The PrP repeats also interact with metal ions, especially Cu(II), which also has suggested roles in prion diseases (70, 71). Although our work does not directly address how such Cu(II)-repeat interactions affect conformational conversion in full-length PrP, it does provide strong evidence that Cu(II) (and Zn(II)) can induce a major conformational rearrangement in the repeats that can affect subsequent amyloid formation. The differential effect of Cu(II) ions on R1+4 *versus* R1+8 may be due to different binding environments of Cu(II) upon assembly (24, 56, 59–61, 72), although non-assembled R1+4 and R1+8 have similar coordination environments indicated by the EPR studies. On the other hand, EPR spectrum broadening was observed for the soluble R1+8 protein, suggesting a dipolar-dipolar interaction, which may result in a very different arrangement of the individual repeat units in R1+8 *versus* in R1+4. Potentially different arrangements of the repeat units could result in different collapse rates and/or stabilities of the oligomeric intermediates. Interestingly, Cu(II) stimulates endocytosis of wild-type PrP^{C} in human neuroblastoma cells, whereas such an event is compromised with expanding the number of the repeats (26). Either deletion or expansion of the repeat region also interferes with Cu(II)-induced association of the PrP repeat region that is fused to a GST protein (17). Thus, more or less than the optimal number of four consecutive repeats results in profound changes in PrP structure and function, and this may be one influence on the high conservation of repeat number during evolution.

Efforts to understand and control the assembly of amyloidogenic proteins are inspired not only by their importance in diverse biological processes, but also their potential applications in nanotechnology (73, 74). NM fibers are stable under a wide variety of conditions and can incorporate a diversity of functions, including the binding of metals that allow them to form nanowires and electronic circuits (74). The NM chimeras with PrP repeats offer new methods for controlling assembly with pH and metal ions, and further raise the possibility of adapting such architectures for novel materials and biotechnological applications. For example, when the chimeras and wild-type NM are mixed together for assembly under different pH, different ratios of the chimeras and NM will be incorporated into individual fibers. If a single cysteine mutation is presented in the chimeras, but not in wild-type NM, different chemical moieties can be introduced via the cysteine on the chimeras but not on wild-type NM. As a result, controlled and fine-tuned patterning and mixing of chemical moieties covalently bound to the mixed fibers can be achieved. This will significantly broaden functional diversity and specificity of these self-assembly-based nanomaterials. In sum, modification of NM by substituting the endogenous repeats with those of PrP has provided insights on assembly that offer additional promise for the future.

Acknowledgments—We thank George Sawicki for performing AFM, Nicki Watson in the Keck Imaging Facility for performing EM, Doug Hattendorf and Rajaraman Krishnan for assistance with protein purification, Susan Uptain for all sorts of helpful advice, Karen Allendoerfer for helpful comments on the manuscript, and all the members of the Millhauser and Lindquist laboratories for their encouragement and support.

REFERENCES

1. Prusiner, S. B. (1998) *Proc. Natl. Acad. Sci. U. S. A.* **95,** 13363–13383
2. Shorter, J., and Lindquist, S. (2005) *Nat. Rev. Genet* **6,** 435–450
3. Patino, M. M., Liu, J. J., Glover, J. R., and Lindquist, S. (1996) *Science* **273,** 622–626
4. Paushkin, S. V., Kushnirov, V. V., Smirnov, V. N., and TerAvanesyan, M. D. (1996) *Embo J.* **15,** 3127–3134
5. Wickner, R. B. (1994) *Science* **264,** 566–569
6. Goldmann, W., Chong, A., Foster, J., Hope, J., and Hunter, N. (1998) *J. Gen. Virol.* **79,** 3173–3176
7. Liu, J. J., and Lindquist, S. (1999) *Nature* **400,** 573–576
8. Chiesa, R., Piccardo, P., Ghetti, B., and Harris, D. A. (1998) *Neuron* **21,** 1339–1351
9. Flechsig, E., Shmerling, D., Hegyi, I., Raeber, A. J., Fischer, M., Cozzio, A., von Mering, C., Aguzzi, A., and Weissmann, C. (2000) *Neuron* **27,** 399–408
10. Bocharova, O. V., Breydo, L., Salnikov, V. V., and Baskakov, I. V. (2005) *Biochemistry-US* **44,** 6776–6787
11. van Rheede, T., Smolenaars, M. M. W., Madsen, O., and de Jong, W. W. (2003) *Mol. Biol. Evol.* **20,** 111–121

12. Goldfarb, L. G., Brown, P., Mccombie, W. R., Goldgaber, D., Swergold, G. D., Wills, P. R., Cervenakova, L., Baron, H., Gibbs, C. J., and Gajdusek, D. C. (1991) *Proc. Natl. Acad. Sci. U. S. A.* **88,** 10926–10930
13. Vital, C., Gray, F., Vital, A., Parchi, P., Capellari, S., Petersen, R. B., Ferrer, X., Jarnier, D., Julien, J., and Gambetti, P. (1998) *Neuropath. Appl. Neuro.* **24,** 125–130
14. Supattapone, S., Bosque, P., Muramoto, T., Wille, H., Aagaard, C., Peretz, D., Nguyen, H. O., Heinrich, C., Torchia, M., Safar, J., Cohen, F. E., DeArmond, S. J., Prusiner, S. B., and Scott, M. (1999) *Cell* **96,** 869–878
15. Legname, G., Baskakov, I. V., Nguyen, H. O., Riesner, D., Cohen, F. E., DeArmond, S. J., and Prusiner, S. B. (2004) *Science* **305,** 673–676
16. Moore, R. A., Herzog, C., Errett, J., Kocisko, D. A., Arnold, K. M., Hayes, S. F., and Priola, S. A. (2006) *Protein Sci.* **15,** 609–619
17. Leliveld, S. R., Dame, R. T., Wuite, G. J., Stitz, L., and Korth, C. (2006) *J. Biol. Chem.* **281,** 3268–3275
18. Shkundina, I. S., Kushnirov, V. V., Tuite, M. F., and Ter-Avanesyan, M. D. (2006) *Genetics* **172,** 827–835
19. Krobitsch, S., and Lindquist, S. (2000) *Proc. Natl. Acad. Sci. U. S. A.* **97,** 1589–1594
20. Scherzinger, E., Lurz, R., Turmaine, M., Mangiarini, L., Hollenbach, B., Hasenbank, R., Bates, G. P., Davies, S. W., Lehrach, H., and Wanker, E. E. (1997) *Cell* **90,** 549–558
21. Kessler, J. C., Rochet, J. C., and Lansbury, P. T. (2003) *Biochemistry-US* **42,** 672–678
22. Barnhart, M. M., and Chapman, M. R. (2006) *Annu. Rev. Microbiol.* **60,** 131–147
23. Chapman, M. R., Robinson, L. S., Pinkner, J. S., Roth, R., Heuser, J., Hammar, M., Normark, S., and Hultgren, S. J. (2002) *Science* **295,** 851–855
24. Millhauser, G. L. (2004) *Accounts Chem. Res.* **37,** 79–85
25. Shiraishi, N., Utsunomiya, H., and Nishikimi, M. (2006) *J. Biol. Chem.* **281,** 34880–34887
26. Perera, W. S., and Hooper, N. M. (2001) *Curr. Biol.* **11,** 519–523
27. Jones, S., Batchelor, M., Bhelt, D., Clarke, A. R., Collinge, J., and Jackson, G. S. (2005) *Biochem. J.* **392,** 309–312
28. Shiraishi, N., Ohta, Y., and Nishikimi, M. (2000) *Biochem. Biophys. Res. Commun.* **267,** 398–402
29. Treiber, C., Pipkorn, R., Weise, C., Holland, G., and Multhaup, G. (2007) *Febs. J.* **274,** 1304–1311
30. Hutter, G., Heppner, F. L., and Aguzzi, A. (2003) *Biol. Chem.* **384,** 1279–1285
31. Sigurdsson, E. M., Brown, D. R., Alim, M. A., Scholtzova, H., Carp, R., Meeker, H. C., Prelli, F., Frangione, B., and Wisniewski, T. (2003) *J. Biol. Chem.* **278,** 46199–46202
32. Shorter, J., and Lindquist, S. (2004) *Science* **304,** 1793–1797
33. Chernoff, Y. O., Lindquist, S. L., Ono, B., Inge-Vechtomov, S. G., and Liebman, S. W. (1995) *Science* **268,** 880–884
34. Parsell, D. A., Kowal, A. S., Singer, M. A., and Lindquist, S. (1994) *Nature* **372,** 475–478
35. Schirmer, E. C., and Lindquist, S. (1997) *Proc. Natl. Acad. Sci. U. S. A.* **94,** 13932–13937
36. Krishnan, R., and Lindquist, S. L. (2005) *Nature* **435,** 765–772
37. Chien, P., DePace, A. H., Collins, S. R., and Weissman, J. S. (2003) *Nature* **424,** 948–951
38. Tanaka, M., Collins, S. R., Toyama, B. H., and Weissman, J. S. (2006) *Nature* **442,** 585–589
39. King, C. Y., and Diaz-Avalos, R. (2004) *Nature* **428,** 319–323
40. Tessier, P. M., and Lindquist, S. (2007) *Nature* **447,** 556–561
41. Sikorski, R. S., and Hieter, P. (1989) *Genetics* **122,** 19–27
42. Scheibel, T., Kowal, A. S., Bloom, J. D., and Lindquist, S. L. (2001) *Curr. Biol.* **11,** 366–369
43. Serio, T. R., and Lindquist, S. L. (1999) *Annual Rev. Cell Dev. Biol.* **15,** 661–703
44. Krebs, M. R. H., Bromley, E. H. C., and Donald, A. M. (2005) *J. Struct. Biol.* **149,** 30–37
45. Glover, J. R., Kowal, A. S., Schirmer, E. C., Patino, M. M., Liu, J. J., and Lindquist, S. (1997) *Cell* **89,** 811–819
46. Chernoff, Y. O., Uptain, S. M., and Lindquist, S. L. (2002) *Methods Enzymol.* **351,** 499–538
47. Derkatch, I. L., Chernoff, Y. O., Kushnirov, V. V., IngeVechtomov, S. G., and Liebman, S. W. (1996) *Genetics* **144,** 1375–1386
48. Tanaka, M., Chien, P., Naber, N., Cooke, R., and Weissman, J. S. (2004) *Nature* **428,** 323–328
49. Uptain, S. M., Sawicki, G. J., Caughey, B., and Lindquist, S. (2001) *EMBO J.* **20,** 6236–6245
50. Tanaka, M., and Weissman, J. S. (2006) *Method Enzymol: Amyloid, Prions, and Other Protein Aggregates* **412,** 185–200
51. Swietnicki, W., Petersen, R., Gambetti, P., and Surewicz, W. K. (1997) *J. Biol. Chem.* **272,** 27517–27520
52. Watanabe, Y., Inanami, O., Horiuchi, M., Hiraoka, W., Shimoyama, Y., Inagaki, F., and Kuwabara, M. (2006) *Biochem. Biophys. Res. Commun.* **350,** 549–556
53. Zou, W. Q., and Cashman, N. R. (2002) *J. Biol. Chem.* **277,** 43942–43947
54. Langella, E., Improta, R., and Barone, V. (2004) *Biophys. J.* **87,** 3623–3632
55. Qin, K. F., Yang, Y., Mastrangelo, P., and Westaway, D. (2002) *J. Biol. Chem.* **277,** 1981–1990
56. Millhauser, G. L. (2007) *Annu. Rev. Phys. Chem.* **58,** 299–320
57. Jackson, G. S., Murray, I., Hosszu, L. L. P., Gibbs, N., Waltho, J. P., Clarke, A. R., and Collinge, J. (2001) *Proc. Natl. Acad. Sci. U. S. A.* **98,** 8531–8535
58. Stockel, J., Safar, J., Wallace, A. C., Cohen, F. E., and Prusiner, S. B. (1998) *Biochemistry-US* **37,** 7185–7193
59. Burns, C. S., Aronoff-Spencer, E., Legname, G., Prusiner, S. B., Antholine, W. E., Gerfen, G. J., Peisach, J., and Millhauser, G. L. (2003) *Biochemistry-US* **42,** 6794–6803
60. Chattopadhyay, M., Walter, E. D., Newell, D. J., Jackson, P. J., Aronoff-Spencer, E., Peisach, J., Gerfen, G. J., Bennett, B., Antholine, W. E., and Millhauser, G. L. (2005) *J. Am. Chem. Soc.* **127,** 12647–12656
61. Burns, C. S., Aronoff-Spencer, E., Dunham, C. M., Lario, P., Avdievich, N. I., Antholine, W. E., Olmstead, M. M., Vrielink, A., Gerfen, G. J., Peisach, J., Scott, W. G., and Millhauser, G. L. (2002) *Biochemistry* **41,** 3991–4001
62. Salnikova, A. B., Kryndushkin, D. S., Smirnov, V. N., Kushnirov, V. V., and Ter-Avanesyan, M. D. (2005) *J. Biol. Chem.* **280,** 8808–8812
63. True, H. L., Berlin, I., and Lindquist, S. L. (2004) *Nature* **431,** 184–187
64. True, H. L., and Lindquist, S. L. (2000) *Nature* **407,** 477–483
65. Serio, T. R., Cashikar, A. G., Kowal, A. S., Sawicki, G. J., Moslehi, J. J., Serpell, L., Arnsdorf, M. F., and Lindquist, S. L. (2000) *Science* **289,** 1317–1321
66. Mukhopadhyay, S., Krishnan, R., Lemke, E. A., Lindquist, S., and Deniz, A. A. (2007) *Proc. Natl. Acad. Sci. U. S. A.* **104,** 2649–2654
67. Shewmaker, F., Wickner, R. B., and Tycko, R. (2006) *Proc. Natl. Acad. Sci. U. S. A.* **103,** 19754–19759
68. Caughey, B., and Raymond, G. J. (1991) *J. Biol. Chem.* **266,** 18217–18223
69. Borchelt, D. R., Taraboulos, A., and Prusiner, S. B. (1992) *J. Biol. Chem.* **267,** 16188–16199
70. Orem, N. R., Geoghegan, J. C., Deleault, N. R., Kascsak, R., and Supattapone, S. (2006) *J. Neurochem.* **96,** 1409–1415
71. Lehmann, S. (2002) *Curr. Opin. Chem. Biol.* **6,** 187–192
72. del Pino, P., Andreas, W., Bertsch, U., Renner, C., Mentler, M., Grantner, K., Fiorino, F., Meyer-Klaucke, W., Moroder, L., Kretzschmar, H. A., and Parak, F. G. (2007) *Eur. Biophys. J.* **36,** 239–252
73. Scheibel, T. (2005) *Curr. Opin. Biotechnol.* **16,** 427–433
74. Scheibel, T., Parthasarathy, R., Sawicki, G., Lin, X. M., Jaeger, H., and Lindquist, S. L. (2003) *Proc. Natl. Acad. Sci. U. S. A.* **100,** 4527–4532

Supplemental Information

PROBING THE ROLE OF PRP REPEATS IN CONFORMATIONAL CONVERSION AND AMYLOID ASSEMBLY OF CHIMERIC YEAST PRIONS*

Jijun Dong[1, 2], Jesse D. Bloom[3†], Vladimir Goncharov[1‡], Madhuri Chattopadhyay[4], Glenn Millhauser[4], David G. Lynn[2], Thomas Scheibel[5], and Susan Lindquist[1]

From [1] Whitehead Institute for Biomedical Research, Cambridge, MA USA, [2] Department of Chemistry and Biology, Emory University, Atlanta, GA USA, [3] Howard Hughes Medical Institute, Department of Molecular Genetics and Cell Biology, University of Chicago, Chicago, IL USA, [4] Department of Chemistry and Biochemistry, University of California, Santa Cruz, CA, USA, [5] Institut für Organische Chemie und Biochemie, Technische Universität München, Garching, [†] Current address: Division of Chemistry and Chemical Engineering, California Institute of Technology, Pasadena, CA, USA [‡]Current address: Francis Bitter Magnet Laboratory/MIT, Cambridge, MA, USA

Running head: amyloid assembly of PrP octarepeats fused to yeast prion protein

Address correspondence to: Dr. Susan Lindquist, Whitehead Institute for Biomedical Research, Cambridge, MA 02142-1479 USA. Phone: 617-258-5184; Fax: 617-258-7226; E-mail: lindquist_admin@wi.mit.edu

Figure S1: AFM images of amyloid fibers formed by the NM domains of wild type Sup35p, R1+4, R1+8, and R1+8H1Q. The fibers formed spontaneously when protein was diluted in PBS and left undisturbed for a period of one week. The protein concentration of the fibers in the images was 2.5 μM, but similar fibers were formed with concentrations ranging from 0.1 to 25 μM. The amount of amorphous aggregates depended on the buffer strength and salt concentration as well as the presence of contaminating proteins. Fibrils in all reactions displayed a similar morphology of long unbranched filaments with uniform diameter.

Figure S2: SDS resistance assays show that acidic pH has different effects on the lag time of fiber formation of wild type NM, R1+4, R1+8 and R1+8H1Q. The gels show the samples from 12.5% SDS-PAGE gels, indicating the fraction of the protein that remains soluble at the given time. Samples in the first lane were boiled, while the others are unboiled. Protein concentration was ~5 μM, and the reactions were stopped by adding the protein loading buffer. Gels are stained with Coomasie Blue.

Figure S3: SDS resistance assays show that acidic pH inhibits fiber formation only of proteins containing histidines in the repeat region. The gels show the unboiled samples from 12.5% SDS-PAGE gels, indicating the fraction of the protein that remains soluble at the given time.

Figure S4: AFM images of amyloid fibers formed by the NM domains of wild type Sup35p, R1+4, R1+8, and R1+8H1Q, in the absence and presence of Cu(II). The fibers formed spontaneously when protein was diluted in 1xCRBB buffer and left undisturbed for a period of one week. The protein concentration of the fibers in the images was 5 μM and metal ions were added in 10 equivalents for R1+4 and NM and in 20 equivalents for all other proteins.

Figure S5: SDS resistance assays of amyloid formation of wild type NM, R1+4, R1+8 and R1+8H1Q, in the presence and absence of different metal ions (Cu(II), Zn(II) and Mn(II)). The gels show samples from 12.5% SDS-PAGE gels, indicating the fraction of the protein that remains soluble at the given time. Samples in the first lane were boiled, while the others are unboiled. Protein concentration at zero hour was 5 μM, and samples were diluted 4:1 by 4X protein loading buffer and 15 μL was loaded in each lane. Gels are stained with Coomasie Blue. The band images were shown on the left, while the normalized band intensities as a function of time were shown on the right.

Figure S1

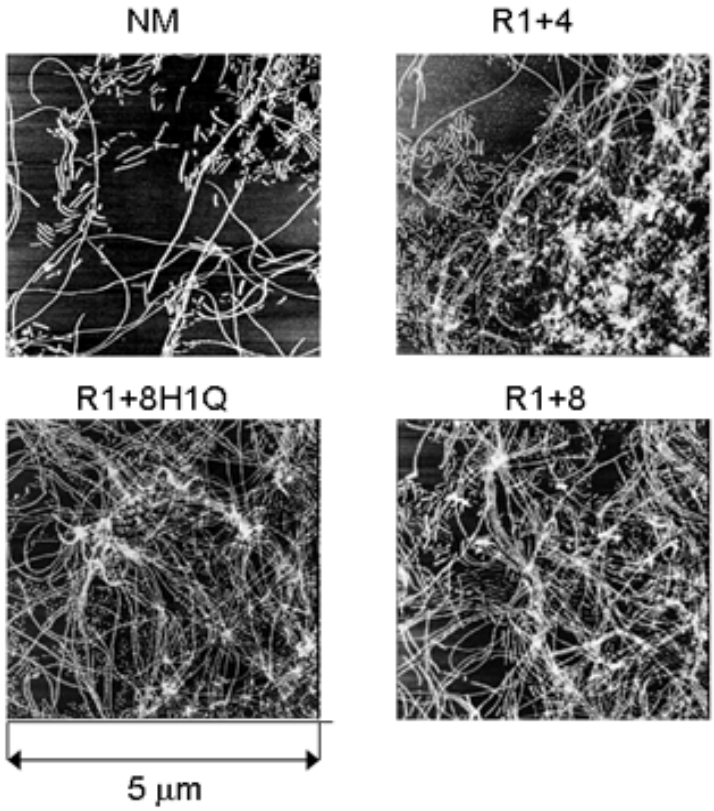

Figure S2

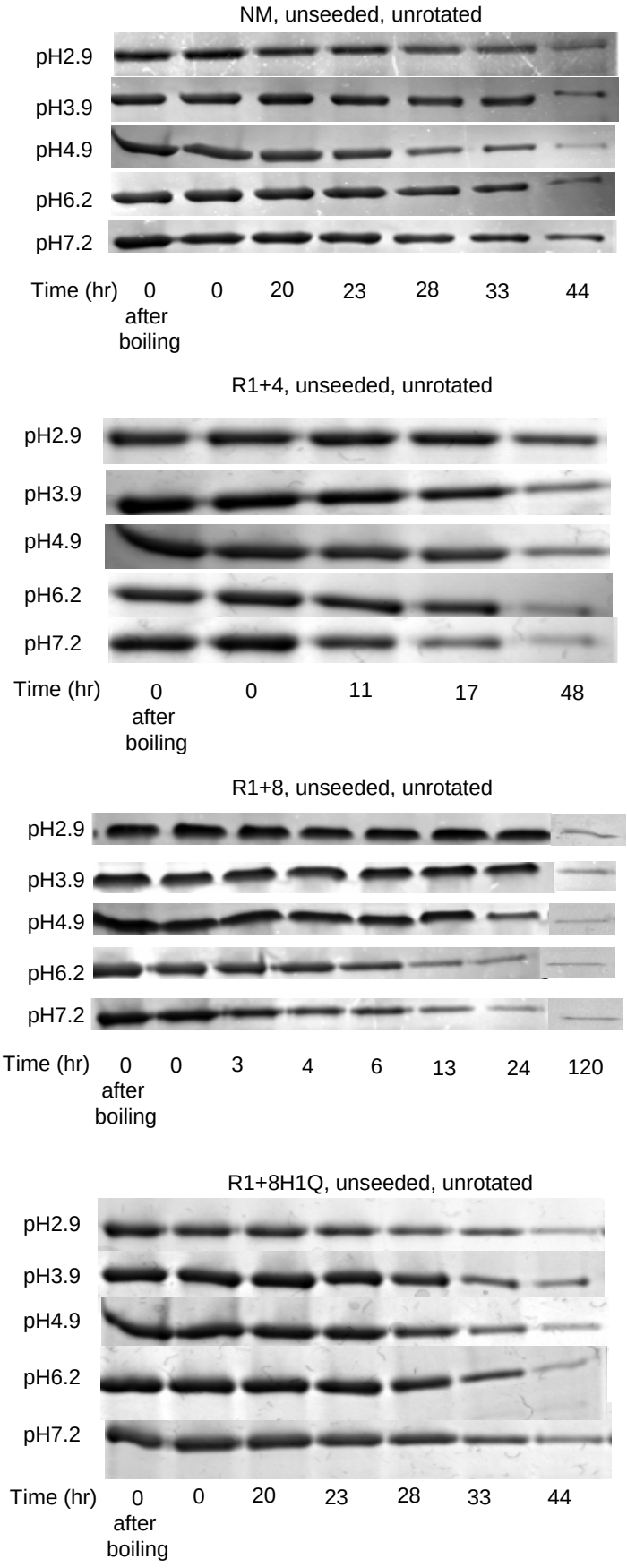
NM, unseeded, unrotated
pH2.9
pH3.9
pH4.9
pH6.2
pH7.2
Time (hr) 0 0 20 23 28 33 44
after boiling
R1+4, unseeded, unrotated
pH2.9
pH3.9
pH4.9
pH6.2
pH7.2
Time (hr) 0 0 11 17 48
after boiling
R1+8, unseeded, unrotated
pH2.9
pH3.9
pH4.9
pH6.2
pH7.2
Time (hr) 0 0 3 4 6 13 24 120
after boiling
R1+8H1Q, unseeded, unrotated
pH2.9
pH3.9
pH4.9
pH6.2
pH7.2
Time (hr) 0 0 20 23 28 33 44
after boiling

Figure S3

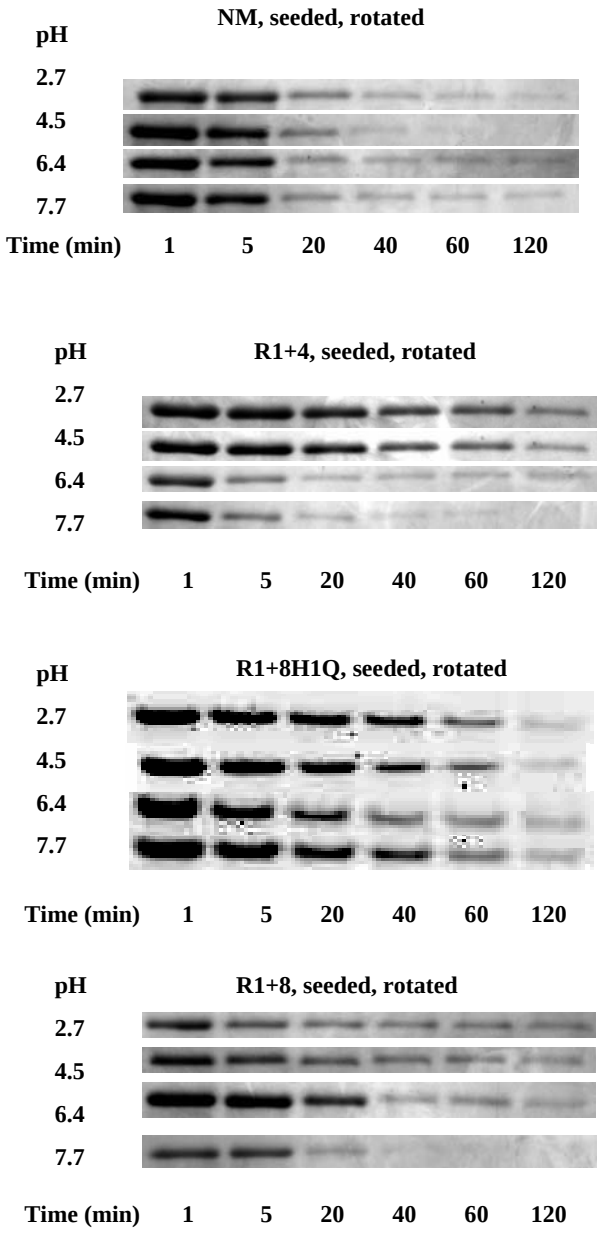
NM, seeded, rotated
pH
2.7
4.5
6.4
7.7
Time (min) 1 5 20 40 60 120
pH
R1+4, seeded, rotated
2.7
4.5
6.4
7.7
Time (min) 1 5 20 40 60 120
pH
R1+8H1Q, seeded, rotated
2.7
4.5
6.4
7.7
Time (min) 1 5 20 40 60 120
pH
R1+8, seeded, rotated
2.7
4.5
6.4
7.7
Time (min) 1 5 20 40 60 120

Figure S4

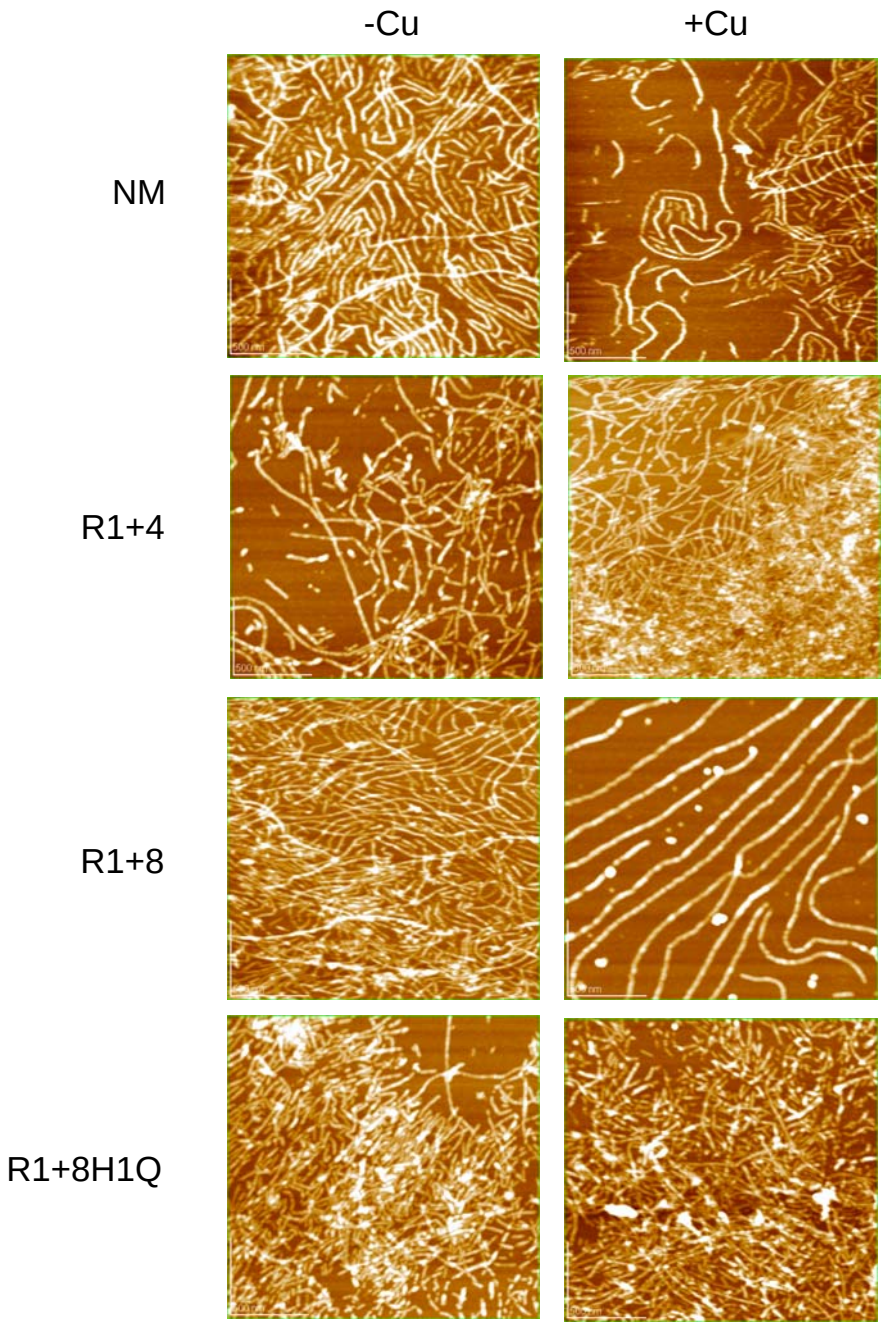

Figure S5

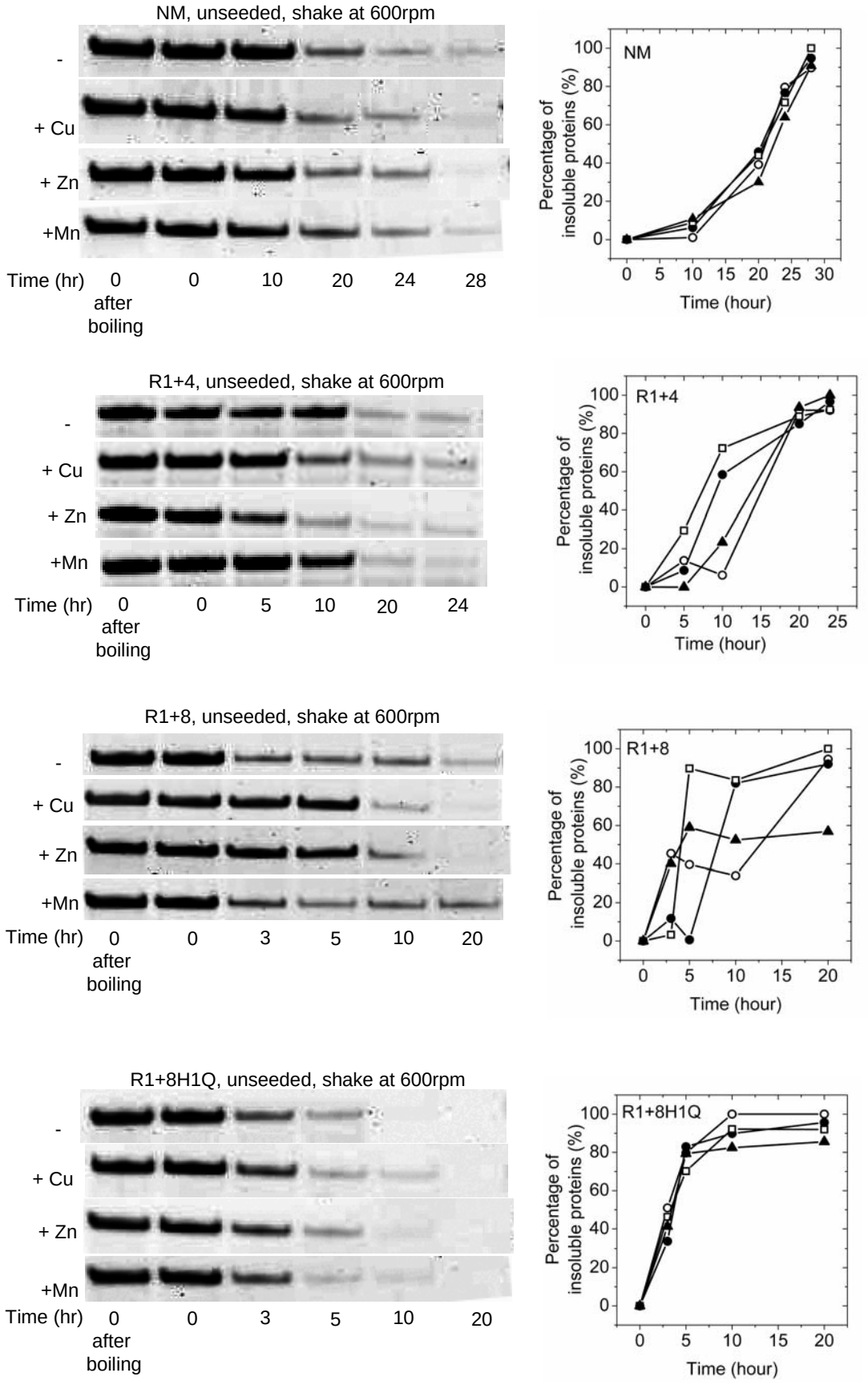
NM, unseeded, shake at 600rpm
-
+ Cu
+ Zn
+Mn
Time (hr) 0 0 10 20 24 28
after boiling
NM
Percentage of insoluble proteins (%)
Time (hour)
R1+4, unseeded, shake at 600rpm
-
+ Cu
+ Zn
+Mn
Time (hr) 0 0 5 10 20 24
after boiling
R1+4
Percentage of insoluble proteins (%)
Time (hour)
R1+8, unseeded, shake at 600rpm
-
+ Cu
+ Zn
+Mn
Time (hr) 0 0 3 5 10 20
after boiling
R1+8
Percentage of insoluble proteins (%)
Time (hour)
R1+8H1Q, unseeded, shake at 600rpm
-
+ Cu
+ Zn
+Mn
Time (hr) 0 0 3 5 10 20
after boiling
R1+8H1Q
Percentage of insoluble proteins (%)
Time (hour)